

# Journal of Materials Chemistry C

Accepted Manuscript



This is an *Accepted Manuscript*, which has been through the Royal Society of Chemistry peer review process and has been accepted for publication.

*Accepted Manuscripts* are published online shortly after acceptance, before technical editing, formatting and proof reading. Using this free service, authors can make their results available to the community, in citable form, before we publish the edited article. We will replace this *Accepted Manuscript* with the edited and formatted *Advance Article* as soon as it is available.

You can find more information about *Accepted Manuscripts* in the [Information for Authors](#).

Please note that technical editing may introduce minor changes to the text and/or graphics, which may alter content. The journal's standard [Terms & Conditions](#) and the [Ethical guidelines](#) still apply. In no event shall the Royal Society of Chemistry be held responsible for any errors or omissions in this *Accepted Manuscript* or any consequences arising from the use of any information it contains.

## Near infrared photoluminescence of the univalent bismuth impurity center in leucite and pollucite crystal hosts.

A.N. Romanov,<sup>a</sup> A.A. Veber,<sup>b</sup> D.N. Vtyurina,<sup>a</sup> Z.T. Fattakhova,<sup>a</sup> E.V. Haula,<sup>a</sup> D.P. Shashkin,<sup>a</sup> V.B. Sulimov,<sup>c</sup> V.B. Tsvetkov,<sup>d</sup> V.N. Korchak<sup>a</sup>

<sup>a</sup> *N.N. Semenov Institute of Chemical Physics, Russian Academy of Sciences, 4 Kosygina Str., 119991 Moscow, Russia*

<sup>b</sup> *Universität Erlangen-Nürnberg, Lehrstuhl für Glas und Keramik, Martensstr. 5, 91058 Erlangen, Germany*

<sup>c</sup> *Research Computer Center of M.V. Lomonosov Moscow State University, 1 Leninskie Gory, Build. 4, 119992 Moscow, Russia*

<sup>d</sup> *A.M. Prokhorov General Physics Institute, Russia Academy of Sciences, 38 Vavilov Str., 119991, Moscow, Russia*

### Abstract

The bismuth doped aluminosilicate phases leucite ( $\text{KAlSi}_2\text{O}_6$ ), gallium leucite ( $\text{KGaSi}_2\text{O}_6$ ) and pollucite ( $\text{CsAlSi}_2\text{O}_6$ ) display the broadband NIR photoluminescence. The active center, responsible for this luminescence is  $\text{Bi}^+$  monocation, which substitutes for the large alkali metal cations. The Al, Si – disorder in aluminosilicate framework of studied crystal phases results in the heterogeneity of  $\text{Bi}^+$  luminescent center population, which manifest itself in the characteristic dependency of luminescence spectrum shape on the excitation wavelength. The relation of NIR emission in  $\text{Bi}^+$ -doped leucite and pollucite phases to the luminescent properties of bismuth-doped glasses is also discussed.

### Introduction

Since the discovery of the broadband near-infrared (NIR) photoluminescence from bismuth doped glasses<sup>1-5</sup> and crystalline materials<sup>6-19</sup> the nature of corresponding luminescent species is widely discussed. The  $\text{Bi}^{3+}$  ion in common oxidation state +3 have not optical transitions in NIR and the observed emission was attributed to possible  $\text{Bi}^{+5}$ ,<sup>1</sup>  $\text{Bi}^{+2}$ ,<sup>20</sup>  $\text{Bi}^{+}$ ,<sup>21</sup>  $\text{Bi}^0$ ,<sup>8,9,22</sup>  $\text{Bi}_2^-$ ,  $\text{Bi}_2^{-2}$ ,<sup>23</sup> and bismuth clusters species<sup>24</sup>. The relating information was also summarized in the recent review<sup>25</sup>. Now it is quite accepted that low-valent (subvalent) bismuth species with Bi oxidation state less than +3 are responsible for NIR emission<sup>26-28</sup>. A lot of subvalent bismuth polycations was known since 1960's and the broadband NIR and

even mid-infrared luminescence from  $\text{Bi}_5^{3+}$  and  $\text{Bi}_8^{2+}$  polycations had been discovered recently<sup>29-33</sup>. It is interesting that NIR luminescence had been detected also from bismuth dimer anion  $\text{Bi}_2^{2-}$  in  $(\text{K-crypt})_2\text{Bi}_2$  crystal phase<sup>34</sup>.

It was also demonstrated, that the univalent bismuth cation  $\text{Bi}^+$  is the NIR emitter in the ternary halide crystals  $\text{KAlCl}_4$ ,  $\text{KMgCl}_3$ ,  $\text{RbPb}_2\text{Cl}_5$ ,  $\text{CsCdCl}_3$ ,<sup>14,17,18,35,36</sup> where  $\text{Bi}^+$  substitutes isomorphically for the large alkali cations. On the other hand, it seems that several different emitters contribute to the net NIR photoluminescence in Bi-doped  $\text{SiO}_2$  and  $\text{GeO}_2$  - based glasses<sup>37,38</sup>. To understand the origin of NIR photoluminescence in Bi-containing silicate and germanate glasses, the investigation of model  $\text{SiO}_2$  or  $\text{GeO}_2$ -based crystals, doped with bismuth is highly desirable, since crystal hosts offer more restrictive and structured environment for the possible bismuth-containing luminescent species. This aspect can diminish the diversity of possible luminescent centers, simplifying the interpretation of photoluminescence spectra. Sun et al. studied the incorporation of NIR-luminescent subvalent bismuth centers into the zeolite Y cages<sup>11-13</sup>. They had postulated the existence of several NIR emitters ( $\text{Bi}^+$  and its oligomers  $\text{Bi}_2^{2+}$ ,  $\text{Bi}_3^{3+}$ ,  $\text{Bi}_4^{4+}$ ) in this system, since the cages of zeolite Y permit the insertion of large bismuth polycations. Probably, the more restrictive crystalline hosts are desirable to isolate the individual Bi-containing emissive centers and explore its optical properties.

Here we set as a goal to prepare the NIR-luminescent bismuth-doped aluminosilicate crystals, where  $\text{Bi}^+$  monocation can be the solely emissive center. Investigation of such crystals can elucidate greatly the possible contribution of  $\text{Bi}^+$  species into the complex NIR luminescence of bismuth-doped aluminosilicate glasses. Also, these materials can be the perspective for photonics on its own, since, contrary to the glasses, they contains only one well defined NIR optical center. Taking into account, that  $\text{Bi}^+$  monocation can isomorphically substitute for the large alkali ions  $\text{K}^+$  and  $\text{Cs}^+$  we explore here the preparation and NIR luminescence of  $\text{Bi}^+$ -substituted  $\text{KAlSi}_2\text{O}_6$ ,  $\text{KGaSi}_2\text{O}_6$  leucites and  $\text{CsAlSi}_2\text{O}_6$  pollucite polycrystalline materials.

### Materials and methods.

All the glasses and crystalline specimens were produced in Nabertherm HTCT 01/16 and RHTC 80-230/15 furnaces in air or nitrogen atmosphere.

Although the  $\text{KAlSi}_2\text{O}_6$  leucite melts congruently at  $1686^\circ\text{C}$ <sup>39</sup>, the direct preparation of this phase by crystallization from the stoichiometric melt of  $\text{K}_2\text{CO}_3$  (as the source of  $\text{K}_2\text{O}$ ),  $\text{Al}_2\text{O}_3$  and  $\text{SiO}_2$  is impeded by the high melting temperature, sufficient melt viscosity and  $\text{K}_2\text{O}$

volatility at elevated temperatures. That's why we prefer to investigate the crystallization of leucite ( $\text{KAlSi}_2\text{O}_6$ ) – diopside ( $\text{MgCaSi}_2\text{O}_6$ ) binary composition. It is known, that leucite-diopside system is of simple eutectic type with leucite primary crystallization field in 100-40 mol % range<sup>39</sup>. We choose the composition 60 leucite - 40 diopside molar parts as the basic, because of its reasonable liquidus temperature ( $\sim 1420^\circ\text{C}$ ), moderate viscosity and easy leucite crystallization. The initial batch was prepared from stoichiometric (relative to 60 leucite - 40 diopside molar parts composition) amounts of  $\text{K}_2\text{CO}_3$ ,  $\text{Al}_2\text{O}_3$ ,  $\text{MgO}$ ,  $\text{CaCO}_3$  and  $\text{SiO}_2$ . Five molar part of  $\text{Bi}_2\text{O}_3$  had been added to this 60 leucite – 40 diopside formulation giving the working composition (60Leu40Dio5Bi thereafter). The starting compounds were grounded in agate mortar, heated to  $1000^\circ\text{C}$ , grounded again and melted at  $1550^\circ\text{C}$  in air for 15 minutes in closed alumina crucible. The melt was cooled quickly on air forming the clear amber-colored glass. The crystallization can be induced by heating of the bulk glass material at temperatures from 1400 to  $1200^\circ\text{C}$  for 20-60 minutes in nitrogen atmosphere. The crystallized specimens were usually quenched in water. After the crystallization the specimens became opaque and gray in appearance. The existence of leucite phase after the crystallization was demonstrated by XRD (Fig. 1a). The well shaped dendrite crystals of the leucite sometimes formed at the surface of the specimen.

The gallium substituted leucite  $\text{KGaSi}_2\text{O}_6$  is known<sup>40</sup> and, although its melting point was not reported earlier, we had expected, that it will be lower, then for its aluminum counterpart. Indeed, it was possible to prepare rather clear glasses by quenching in air the composition  $20\text{KGaSi}_2\text{O}_6 - 1\text{Bi}_2\text{O}_3$ , melted at  $1550^\circ\text{C}$ . The initial batch was composed from the stoichiometric amounts of  $\text{K}_2\text{CO}_3$ ,  $\text{Ga}_2\text{O}_3$ ,  $\text{SiO}_2$  and  $\text{Bi}_2\text{O}_3$ , it was thoroughly grounded in mortar, calcined at  $900^\circ\text{C}$  and finally melted for 15-20 minutes at  $1550^\circ\text{C}$ . The subsequent crystallization of the glasses in nitrogen at  $1250^\circ\text{C}$  afforded opaque crystalline material with characteristic leucite XRD diagram (Fig. 1b).

The pollucite phase  $\text{CsAlSi}_2\text{O}_6$  is the most refractory silicate known with melting point above  $1900^\circ\text{C}$ <sup>41</sup>. That's why the bismuth-doped pollucite phases with different Bi doping concentrations were prepared with the aid of  $\text{B}_2\text{O}_3$  flux. The initial batches with varying bismuth contents  $14\text{CsNO}_2-7\text{Al}_2\text{O}_3-28\text{SiO}_2-12\text{H}_3\text{BO}_3-(0.233; 0.7; 2.1)\text{Bi}_2\text{O}_3$  was chosen to give the corresponding  $7\text{CsAlSi}_2\text{O}_6-3\text{B}_2\text{O}_3-x\text{Bi}_2\text{O}_3$  ( $x = 0.117; 0.35; 1.05$ ) final melt compositions when pollucite had formed and all volatiles were evaporated. The constituents were mixed in agate mortar, calcined at  $1000^\circ\text{C}$ , grounded again, melted at  $1550^\circ\text{C}$  for 15 min then cooled to  $1100^\circ\text{C}$  for 4 min. At this temperature the specimens were quenched in water. The clear glass is not formed in this case and the XRD analysis reveals the peaks from

pollucite along with diffuse halo from remaining glass phase. Since the pollucite is more stable toward acid and base attack than leucite it was possible to refine it from the remaining borate glass phase by subsequent treatment of finely powdered sample with boiling KOH solution (1 hour) and diluted HNO<sub>3</sub> (5 min) at room temperature. This treatment practically eliminates the intensity of halo in XRD spectra, leaving clear pollucite diffraction peaks (Fig. 1c) and also (as will be discussed below) eliminates the broad bismuth NIR luminescence spectrum, characteristic for Bi-doped glass phase. To our knowledge, this is the first report of CsAlSi<sub>2</sub>O<sub>6</sub> pollucite phase crystallization from B<sub>2</sub>O<sub>3</sub> flux.

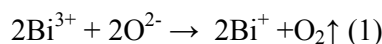
The spectra of NIR photoluminescence, luminescence excitation and 2D excitation-emission spectra along with photoluminescence kinetic characteristics were obtained at room temperature as described earlier<sup>17,18,35,36</sup>.

Several CW diode and DPSS lasers with wavelengths 450 nm, 470 nm, 532 nm, 635 nm, 660 nm and 690 nm and 20-200 mW output power were employed to excite the photoluminescence.

XRD characterization was afforded with DRON-3 X-ray diffractometer.

## Results and discussion

It was described above, that bismuth doped compositions 60Leu40Dio5Bi and 20KGaSi<sub>2</sub>O<sub>6</sub> – 1 Bi<sub>2</sub>O<sub>3</sub> can be obtained in two forms: as quenched clear glass or crystallized specimens, containing KAlSi<sub>2</sub>O<sub>6</sub> or KGaSi<sub>2</sub>O<sub>6</sub> leucite phases along with residual glass. The respective quenched glasses exhibit the broad NIR photoluminescence, characteristic for bismuth containing SiO<sub>2</sub>-based glasses (Fig. 2,3). The shape of the photoluminescence spectra depends on the excitation wavelength, although their maxima positions is nearly identical for λ<sub>ex</sub>=470 nm and λ<sub>ex</sub>=532 nm: λ<sub>max</sub>=1230 nm for 60Leu40Dio5Bi glass and λ<sub>max</sub>=1247 nm for 20KGaSi<sub>2</sub>O<sub>6</sub> – 1 Bi<sub>2</sub>O<sub>3</sub> glass. It is quite accepted now, that broadband NIR luminescence in these glasses were resulted from several subvalent bismuth species, which are generated from Bi<sup>3+</sup> by the thermal reductive disproportionation (shown below for Bi<sup>+</sup> generation):



At sufficiently high temperatures the oxygen partial pressure, generated by process (1) overwhelm the oxygen concentration in atmosphere, and subvalent bismuth species can be formed by melting of bismuth-containing compositions in the open air.

Upon glass crystallization of the both compositions 60Leu40Dio5Bi and 20KGaSi<sub>2</sub>O<sub>6</sub> – 1Bi<sub>2</sub>O<sub>3</sub> the dramatic changes in NIR luminescence spectra had occurred: the luminescence peaks became much sharper (although still rather broad) at every excitation wavelength (Fig.

2,3) and blue-shifted relative to the corresponding glasses. The dependency of the photoluminescence spectra shape on the excitation wavelength is more pronounced in these crystallized specimens ( $\lambda_{\text{max}}=1188$  nm at  $\lambda_{\text{ex}}=470$  nm and  $\lambda_{\text{max}}=1170$  nm at  $\lambda_{\text{ex}}=532$  nm for 60Leu40Dio5Bi glass whereas  $\lambda_{\text{max}}=1202$  nm at  $\lambda_{\text{ex}}=470$  nm and  $\lambda_{\text{max}}=1170$  nm at  $\lambda_{\text{ex}}=532$  nm for 20KGaSi<sub>2</sub>O<sub>6</sub> – 1 Bi<sub>2</sub>O<sub>3</sub>).

This marked change of the luminescence spectrum upon glass crystallization can be rationalized as possible interplay of two factors: (i) the initial glass contains many kinds of bismuth NIR luminescent centers, but due to the steric restrictions, only the limited number of such centers (or even one center) can be incorporated into crystal phase after glass crystallization, resulting in the simplification of luminescence spectrum (ii) the spectrum became sharper after the NIR luminescent center transition from disordered (glass) to ordered (crystal) phase.

The photoluminescence spectra of crystallized 20KGaSi<sub>2</sub>O<sub>6</sub> – 1 Bi<sub>2</sub>O<sub>3</sub> specimen contains only weak long-wavelength tails (above 1400 nm), whereas in 60Leu40Dio5Bi specimen these tails are prominent. It is reasonable to consider, that these tails originate from the luminescence of the residual glassy phase. Indeed, the crystallized 60Leu40Dio5Bi specimen should contain large amount of the residual glass, since we did not observe the indications of massive diopside crystallization from this glass (Fig. 1a). So, the most of diopside in this composition should remain glassy.

For the resulted crystalline phases KAlSi<sub>2</sub>O<sub>6</sub> and KGaSi<sub>2</sub>O<sub>6</sub> we can assume, that due to the large crystal ionic radius for the bismuth ion species, the only cation, which can be substituted by NIR luminescent bismuth center is K<sup>+</sup>. To verify this assumption we synthesize (by the procedure, similar to the preparation of 60Leu40Dio5Bi and 20KGaSi<sub>2</sub>O<sub>6</sub> – 1Bi<sub>2</sub>O<sub>3</sub> specimens) the bismuth doped glasses with pure diopside and spodumene (LiAlSi<sub>2</sub>O<sub>6</sub>) compositions, which can be crystallized to the respective crystalline phases. Whereas the diopside and spodumene glasses demonstrated the broadband NIR luminescence, the crystalline diopside and spodumene, resulted from crystallization of these glasses was completely devoid of NIR photoluminescence or demonstrated only weak luminescence similar to the glassy specimens (probably, from the residual glassy phase). This circumstance necessitate to assume, that NIR luminescent bismuth centers can substitute only for the large K<sup>+</sup> cations in KAlSi<sub>2</sub>O<sub>6</sub> and KGaSi<sub>2</sub>O<sub>6</sub> aluminosilicates, but not for the relatively small Li, Al or Si ions.

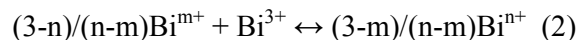
We also succeeded in the preparation of bismuth-doped pollucite from B<sub>2</sub>O<sub>3</sub>-containing flux. As the crystal structures of pollucite and leucite are similar it is no wonder

that the NIR luminescence spectra from Bi-doped pollucite are also similar to the Bi-doped leucites (Fig. 4). Also, the Bi-doped pollucite can be prepared in form, sufficiently pure from the remaining non crystallized glassy phase, which makes it the convenient materials for the study of Bi-doped NIR luminescence in the crystal aluminosilicates.

One prominent feature of NIR luminescence from Bi-doped leucites and pollucite is the marked dependence of luminescence spectra on the excitation wavelength (Fig. 4, for pollucite  $\lambda_{\text{max}}=1196$  nm at  $\lambda_{\text{ex}}=405$  nm,  $\lambda_{\text{max}}=1170$  nm at  $\lambda_{\text{ex}}=532$  nm,  $\lambda_{\text{max}}=1066$  nm at  $\lambda_{\text{ex}}=635$  nm,  $\lambda_{\text{max}}=1074$  nm at  $\lambda_{\text{ex}}=660$  nm and  $\lambda_{\text{max}}=1090$  nm at  $\lambda_{\text{ex}}=690$  nm). This dependence implies that several different bismuth-containing luminescent centers are present in the studied aluminosilicate phases. To elucidate the nature of these centers we had prepared the pollucite phases with different amounts of bismuth oxide in the starting mixtures. We found that the increased proportion of bismuth oxide in the batch intensifies the NIR luminescence of the prepared pollucite phase. In fact, the intensities of photoluminescence from the three pollucite specimens, prepared with the aid of fluxes with different bismuth contents relates as 1:2.2:7.4 (with excitation at 532 nm). This correspond roughly to the ratio of bismuth content (1:3:9) in the starting mixture – the deviation can be resulted from bismuth evaporation from the flux. This fact signifies that the increased amount of bismuth in the batch leads to the pollucite specimens, containing more bismuth luminescent centers. It is interesting, that the overall shape of the luminescence spectra (measured at different excitation wavelengths) is independent on the concentration of luminescent centers in pollucite. So, the photoluminescence spectra, excited at specified wavelength for specimens with different amount of  $\text{Bi}_2\text{O}_3$  in initial batch can be perfectly superimposed upon one another (Fig. 5). This is in sharp contrast with the properties of Bi-related NIR luminescence from  $\text{SiO}_2$ -based glasses, where the variation of  $\text{Bi}_2\text{O}_3$  concentration markedly affects the shape of luminescence spectrum<sup>42-44</sup>.

These independence of luminescence spectra shape on bismuth concentration in the melt (represented by  $\text{Bi}^{3+}$  and also by subvalent Bi species) signify, that although the prepared pollucite phases contains the several Bi-containing luminescent centers which are all contribute to the net luminescence spectrum, their relative proportion are independent on their concentrations and also on concentration of  $\text{Bi}^{3+}$  as the prevalent bismuth oxidation state in the melt. This independency means that unlike the Bi-doped glasses, multiple luminescent centers in Bi-doped pollucite should have the similar oxidation state and the number of bismuth atoms.

Indeed, if the luminescent centers would have the different oxidation states (for example  $+m$  and  $+n$ ,  $m \neq n$ ,  $m \neq 3$ ,  $n \neq 3$ ), their relative proportion should be affected by  $\text{Bi}^{3+}$  concentration via the equilibrium reaction:



Also, if the luminescent centers would have the same oxidation state but different number of bismuth atoms (from dimerization or oligomerization reactions) their relative proportions should depend on their concentrations.

The only explanation for the existence of different luminescent centers with the same oxidation state and number of bismuth atoms is the influence of different crystal field, creating subpopulations of luminescent centers which are essentially the same substance from the chemical point of view but situated in different crystal environment. This is in contrast with the existence of many chemically different oligomeric Bi-containing luminescent species, observed by Sun et al. in zeolite Y<sup>11-13</sup>. The reason, why we had observed only one chemically unique luminescent Bi center is that pollucite structure contains significantly smaller cages in aluminosilicate framework, than zeolite Y. These small cages have not enough space to accommodate the different oligomeric subvalent bismuth species. So, the only monoatomic bismuth cations can be the source of observed NIR luminescence. Since  $\text{Bi}^{3+}$  and  $\text{Bi}^{2+}$  can not emit in NIR and it was shown that monocation  $\text{Bi}^+$  is the NIR emitter in chloride crystals it is reasonable to postulate, that  $\text{Bi}^+$  center is also the source of NIR photoluminescence in Bi-doped pollucite. Recently, we had estimated the crystal ionic radius of  $\text{Bi}^+$  and demonstrated that the isomorphic substitution of  $\text{Cs}^+$  for  $\text{Bi}^+$  is possible<sup>45</sup>, so  $\text{Bi}^+$  can readily incorporate into pollucite framework in place of  $\text{Cs}^+$ .

The varying crystal field parameters at  $\text{Bi}^+$  site, which create the heterogeneity of luminescent center population can result from the positional disorder of Al and Si in aluminosilicate framework of pollucite (and also leucite) structure. In pollucite, the  $\text{Cs}^+$  ion is coordinated by 12 oxygen ions which belong to 15 structural Si or Al tetrahedra. So, there are many possibilities of different random arrangements of Si and Al tetrahedra, around  $\text{Bi}^+$  center, creating the above mentioned heterogeneity of luminescent center population. Also, the off centering of  $\text{Bi}^+$  position in the cage and possible crystal lattice defects can also contribute to the inhomogeneous broadening of luminescence. The disorder in the  $\text{Cs}^+$  ion environment in synthetic pollucite was observed earlier by Ashbrook et al<sup>46</sup>.

As the characteristics of NIR luminescence from Bi-doped leucites mimic the emission properties of Bi-doped pollucite, we suggest, that the model of  $\text{Bi}^+$  NIR luminescent center, which we deduce for pollucite can also be applicable for aluminium and gallium

leucites, where  $\text{Bi}^+$  isomorphically substitute for  $\text{K}^+$ . This suggestion is also strengthened by the data on temporal luminescence decay in Bi-doped gallium leucites, measured at different emission wavelengths. Indeed, we had found that NIR luminescence decay was always single-exponential with lifetimes only slightly varying along emission wavelength range (401-429  $\mu\text{s}$  in seven measurements at wavelengths from 1100 to 1300 nm, Fig. 6). This implies the similar nature of emissive centers for all observed NIR luminescence spectral diapason. Also, the characteristic decay time of NIR luminescence is similar to the other crystal phases<sup>18,35</sup>, doped with  $\text{Bi}^+$ .

Returning to the heterogeneity of  $\text{Bi}^+$  population due to the different crystal environment we can suggest the simple qualitative picture, based on empirical crystal field model of Davis et al<sup>47</sup>.  $\text{Bi}^+$  monocation in free space has the nondegenerate  $^3\text{P}_0$  ground state; triply degenerate lowest excited  $^3\text{P}_1$  level and then quintuple degenerate  $^3\text{P}_2$  level. The crystal field of low symmetry in disordered pollucite lattice split all the degenerate levels and the lowest energy component from  $^3\text{P}_1$  manifold form the level, from which the main radiative transition to the ground state had occurred, causing NIR luminescence. Due to the disordered crystal lattice, the  $\text{Bi}^+$  population is heterogeneous – situated in different crystal environment with varying crystal field strength. The energy gap between the lowest excited level and the ground state became narrow in the relatively strong-field environment due to increased  $^3\text{P}_0$  split (See Fig. 7). So, the red-shifted portions in NIR luminescence spectrum are emitted from relatively strong-field luminescent centers. Optical excitation of NIR luminescence is performed via absorbance at transition  $^3\text{P}_0 \rightarrow ^3\text{P}_2$  to the components of the split  $^3\text{P}_2$  level with subsequent internal conversion to the luminescent level in  $^3\text{P}_1$  manifold. If we scan the excitation wavelength from blue to the red, decreasing the maximal available energy of photoexcited state, we firstly change the selection of excited luminescent centers from strong to weak-field, obtaining the luminescence with progressively decreased wavelengths of maxima (Fig. 7). Then, after passing the excitation wavelength, corresponding to the unperturbed  $^3\text{P}_0 \rightarrow ^3\text{P}_2$  transition (at zero field), the continued red shift in excitation will produce the opposite effect of selecting relatively more strong-field luminescent centers and the wavelength of luminescence maximum begin to increase with the increasing of excitation wavelength. This tendency can be seen in data on Fig. 4. In this manner, the 2D excitation-emission spectra of NIR luminescence can be viewed as the plots of available excitation energy vs. relative crystal field strength, proportional to the emission wavelength. The intensity, shown in these spectra illustrates the distribution of luminescent centers vs. crystal field strength of its environment. The simple qualitative model, explained above should

manifest itself in 2D excitation-emission spectra as the existence of two branches with opposite dependence of emission maxima wavelength on excitation one. These two branches intersect each other at excitation wavelength, corresponding to  $^3P_0 \rightarrow ^3P_2$  optical transition in  $\text{Bi}^+$  luminescent center at zero crystal field. As the population of such weakest-field centers in the specimens is negligible, the intensity of branches nearly vanished at intersect point, and it can be found only by the extrapolation. Such characteristic 2D excitation-emission plot for Bi-doped gallium leucite specimen is shown on Fig. 8. The similar 2D plots are also obtained for different Bi-containing NIR luminescent materials, for example, aluminosilicate glasses at very low Bi-doping level<sup>48</sup>. They also contain the two well-distinguished branches of luminescent signal. This similarity signify, that in aluminosilicate glass at low Bi doping concentrations the monocation  $\text{Bi}^+$  also act as main NIR luminescent emitter and as the lasing substance. In the leucite and pollucite aluminosilicate phases, the large alkali cations (and also luminescent  $\text{Bi}^+$ ) can be considered as the compensators for the negative charge of aluminosilicate framework, introduced by  $[\text{AlO}_{4/2}]^-$  four-coordinate aluminium units. Keeping in mind the similarity of NIR luminescence parameters for the  $\text{Bi}^+$ -containing aluminosilicate crystals and glasses at low Bi-doping level, the NIR luminescent emitter in such glasses can also be considered as the interstitial  $\text{Bi}^+$ , which compensates for the negative charge on the nearby tetrahedral aluminium unit  $[\text{AlO}_{4/2}]^-$  in place of neutral  $[\text{SiO}_{4/2}]$  in  $\text{SiO}_2$  framework. Such  $([\text{AlO}_{4/2}]^-, \text{Bi}^+)$  center was already proposed as the possible NIR emitter (around 1170 nm) in bismuth doped aluminosilicate glass<sup>49</sup>, and bismuth/aluminum codoped zeolite derived glass nanoparticles<sup>50</sup>. The results of present investigation also confirm this hypothesis.

Probably, other subvalent and also emissive centers can be formed in glasses at high bismuth doping level (or without aluminium codoping). These emissive centers can be responsible for the luminescence at relatively long wavelengths, which are also present in leucite glasses, but disappear mainly after crystallization. It was observed earlier, that simultaneous existence of different emitting centers in Bi-doped optical materials can hamper the possible laser generation on each of these centers<sup>51</sup>. So,  $\text{Bi}^+$ -containing aluminosilicate crystals can offer the good possibility for creating the solid state laser media with well-defined active centers.

## Conclusions

In contrast with the glass media, the aluminosilicate leucite and pollucite crystals offer restricted environment to possible subvalent luminescent bismuth centers, so only  $\text{Bi}^+$  monocations are observed as NIR emitting centers at different Bi-doping levels. Despite the

existence of only one chemically unique luminescent center, the NIR emission spectra are still rather broad due to the heterogeneity of Bi<sup>3+</sup> luminescent centers in the disordered aluminosilicate network of pollucite and leucites.

### Acknowledgments

The reported work was supported by Russian Foundation for Basic Research (RFBR, research project number 13-03-00777).

### References

1. Y. Fujimoto and M. Nakatsuka, *Jpn. J. App. Phys.*, 2001, **40**, L279.
2. Y. Fujimoto and M. Nakatsuka, *Appl. Phys. Lett.*, 2003, **82**, 3325.
3. X. Meng, J. Qiu, M. Peng, D. Chen, Q. Zhao, X. Jiang and C. Zhu, *Opt. Express*, 2005, **13**, 1628.
4. X. Meng, J. Qiu, M. Peng, D. Chen, Q. Zhao, X. Jiang and C. Zhu, *Opt. Express*, 2005, **13**, 1635.
5. A.N. Romanov, E.V. Haula, Z.T. Fattakhova, A.A. Veber, V.B. Tsvetkov, D.M. Zhigunov, V.N. Korchak and V.B. Sulimov, *Opt. Mater.*, 2011, **34**, 155.
6. L. Su, J. Yu, P. Zhou, H. Li, L. Zheng, Y. Yang, F. Wu, H. Xia and J. Xu, *Opt. Lett.*, 2009, **34**, 2504.
7. J. Ruan, L. Su, J. Qiu, D. Chen and J. Xu, *Opt. Express*, 2009, **17**, 5163.
8. M. Peng, B. Sprenger, M.A. Schmidt, H.G.L. Schwefel and L. Wondraczek, *Opt. Express*, 2010, **18**, 12852.
9. J. Zheng, M. Peng, F. Kang, R. Cao, Z. Ma, G. Dong, J. Qiu and S. Xu, *Opt. Express*, 2012, **20**, 22569.
10. C. Li, Z. Song, J. Qiu, Z. Yang, X. Yu, D. Zhou, Z. Yin, R. Wang, Y. Xu and Y. Cao, *J. Lumin.*, 2012, **132**, 1807.
11. H.-T. Sun, Y. Matsushita, Y. Sakka, N. Shirahata, M. Tanaka, Y. Katsuya, H. Gao and K. Kobayashi, *J. Am. Chem. Soc.*, 2012, **134**, 2918.
12. H.-T. Sun, Y. Sakka, N. Shirahata, Y. Matsushita, K. Deguchi and T. Shimizu, *J. Phys. Chem. C*, 2013, **117**, 6399.
13. H.-T. Sun, A. Hosokawa, Y. Miwa, F. Shimaoka, M. Fujii, M. Mizuhata, S. Hayashi and S. Deki, *Adv. Mater.*, 2009, **21**, 3694.
14. A.G. Okhrimchuk, L.N. Butvina, E.M. Dianov, N.V. Lichkova, V.N. Zagorodnev and K.N. Boldyrev, *Opt. Lett.*, 2008, **33**, 2182.

15. L. Su, H. Zhao, H. Li, L. Zheng, G. Ren, J. Xu, W. Ryba-Romanowski, R. Lisiecki and P. Solarz, *Opt. Lett.*, 2011, **36**, 4551.
16. L. Su, H. Zhao, H. Li, L. Zheng, X. Fan, X. Jiang, H. Tang, G. Ren, J. Xu, W. Ryba-Romanowski, R. Lisiecki and P. Solarz, *Opt. Mater. Express*, 2012, **2**, 757.
17. A.A. Veber, A.N. Romanov, O.V. Usovich, Z.T. Fattakhova, E.V. Haula, V.N. Korchak, L.A. Trusov, P.E. Kazin, V.B. Sulimov and V.B. Tsvetkov, *Appl. Phys. B*, 2012, **108**, 733.
18. A.N. Romanov, A.A. Veber, Z.T. Fattakhova, O.V. Usovich, E.V. Haula, L.A. Trusov, P.E. Kazin, V.N. Korchak, V.B. Tsvetkov and V.B. Sulimov, *J. Lumin.*, 2013, **134**, 180.
19. V.G. Plotnichenko, V.O. Sokolov, D.V. Philippovskiy, I.S. Lisitsky, M.S. Kouznetsov, K.S. Zaramenskikh and E.M. Dianov, *Opt. Lett.*, 2013, **38**, 362.
20. J. Ren, J. Qiu, D. Chen, C. Wang, X. Jiang and C. Zhu, *J. Mater. Res.*, 2007, **22**, 1954.
21. X. Meng, J. Qiu, M. Peng, D. Chen, Q. Zhao, X. Jiang and C. Zhu, *Opt. Express*, 2005, **13**, 1628.
22. M. Peng, C. Zollfrank and L. Wondraczek, *J. Phys.: Condens. Matter*, 2009, **21**, 285106.
23. V.O. Sokolov, V.G. Plotnichenko, V.V. Koltashev and E.M. Dianov, *J. Phys. D: Appl. Phys.*, 2009, **42**, 095410.
24. M. Peng, J. Qiu, D. Chen, X. Meng and C. Zhu, *Opt. Lett.*, 2005, **30**, 2433.
25. H.-T. Sun, J. Zhou and J. Qiu, *Prog. Mater. Sci.*, 2014, **64**, 1-72.
26. A.S. Zlenko, V.M. Mashinsky, L.D. Iskhakova, S.L. Semjonov, V.V. Koltashev, N.M. Karatun and E.M. Dianov, *Opt. Express*, 2012, **20**, 23186.
27. A.N. Romanov, Z.T. Fattakhova, D.M. Zhigunov, V.N. Korchak and V.B. Sulimov, *Opt. Mater.*, 2011, **33**, 631.
28. H.-T. Sun, Y. Sakka, M. Fujii, N. Shirahata and H. Gao, *Opt. Lett.*, 2011, **36**, 100.
29. H.-T. Sun, Y. Sakka, H. Gao, Y. Miwa, M. Fujii, N. Shirahata, Z. Bai and J.-G. Li, *J. Mater. Chem.*, 2011, **21**, 4060.
30. R. Cao, M. Peng, L. Wondraczek and J. Qiu, *Opt. Express*, 2012, **20**, 2562.
31. R. Cao, M. Peng, J. Zheng, J. Qiu, and Q. Zhang, *Opt. Express*, 2012, **20**, 18505.
32. H.-T. Sun, B. Xu, T. Yonezawa, Y. Sakka, N. Shirahata, M. Fujii, J. Qiu and H. Gao, *Dalton Trans.*, 2012, **41**, 11055.
33. H.-T. Sun, Y. Sakka, N. Shirahata, H. Gao and Tetsu Yonezawa, *J. Mater. Chem.*, 2012, **22**, 12837.

34. H.-T. Sun, T. Yonezawa, M.M. Gillett-Kunnath, Y. Sakka, N. Shirahata, S.C.R. Gui, M. Fujii and S.C. Sevov, *J. Mater. Chem.*, 2012, **22**, 20175.
35. A.N. Romanov, A.A. Veber, Z.T. Fattakhova, D.N. Vtyurina, M.S. Kouznetsov, K.S. Zaramenskikh, I.S. Lisitsky, V.N. Korchak, V.B. Tsvetkov and V.B. Sulimov, *J. Lumin.*, 2014, **149**, 292.
36. A.A. Veber, A.N. Romanov, O.V. Usovich, Z.T. Fattakhova, E.V. Haula, V.N. Korchak, L.A. Trusov, P.E. Kazin, V.B. Sulimov and V.B. Tsvetkov, *J. Lumin.*, 2014, **151**, 247.
37. X. Guo, H. Li, L. Su, P. Yu, H. Zhao, Q. Wang, J. Liu and J. Xu, *Opt. Mater.*, 2012, **34**, 675.
38. I. Razdobreev, H. El Hamzaoui, V.Yu. Ivanov, E.F. Kustov, B. Capoen and M. Bouazaoui, *Opt. Lett.*, 2010, **35**, 1341.
39. N.L. Bowen and J.F. Schairer, *Am. J. Sci.*, 1929, **18**, 301.
40. A.T. Durant, K.J.D. MacKenzie and H. Maekawa, *Dalton Trans.*, 2011, **40**, 4865.
41. W. Holand and G.H. Beall, *Glass-Ceramic Technology*, Second Edition, 2012, The American Ceramic Society, John Wiley and Sons Inc., Hoboken, New Jersey.
42. M.A. Hughes, T. Suzuki and Y. Ohishi, *Opt. Mater.*, 2009, **32**, 368.
43. M.A. Hughes, T. Suzuki and Y. Ohishi, *J. Non-Cryst. Solids*, 2010, **356**, 2302.
44. M. Qian, C. Yu, J. Cheng, K. Li and L. Hu, *J. Lumin.*, 2012, **132**, 2634.
45. A.N. Romanov, F.V. Grigoriev and V.B. Sulimov, *Comput. Theor. Chem.*, 2013, **1017**, 159.
46. S.E. Ashbrook, K.R. Whittle, L. Le Pollès and I. Farnan, *J. Am. Ceram. Soc.*, 2005, **88**, 1575.
47. H.L. Davis, N.J. Bjerrum, G.P. Smith, *Inorg. Chem.*, 1967, **6**, 1172.
48. S.V. Firstov, V.F. Khopin, I.A. Bufetov, E.G. Firstova, A.N. Guryanov, and E.M. Dianov, *Opt. Express*, 2011, **19**, 19551.
49. V.V. Dvoyrin, V.M. Mashinsky, E.M. Dianov, A.A. Umnikov, M.V. Yashkov and A.N. Guryanov, *Proc. 31st European Conference on Optics Communication (ECOC)*, 2005, Glasgow, **4**, 949.
50. H.-T. Sun, T. Hasegawa, M. Fujii, F. Shimaoka, Z. Bai, M. Mizuhata, S. Hayashi and S. Deki, *Opt. Express*, 2009, **17**, 6239.
51. R. Gumenyuk, K. Golant, O.G. Okhotnikov, *Appl. Phys. Lett.*, 2011, **98**, 191108.

**Figure captions**

**Fig.1** X-ray diffraction patterns of crystallized 60Leu40Dio5Bi glass (a), crystallized 20KGaSi<sub>2</sub>O<sub>6</sub> – 1Bi<sub>2</sub>O<sub>3</sub> glass (b) and pollucite phase, crystallized from the melt with 7CsAlSi<sub>2</sub>O<sub>6</sub>-3B<sub>2</sub>O<sub>3</sub>-1.05Bi<sub>2</sub>O<sub>3</sub> composition and refined from the residual flux by subsequent treatment with KOH and HNO<sub>3</sub> (c). All the noticeable peaks are from leucite (KAlSi<sub>2</sub>O<sub>6</sub>), gallium leucite (KGaSi<sub>2</sub>O<sub>6</sub>) and pollucite (CsAlSi<sub>2</sub>O<sub>6</sub>) phases.

**Fig.2** Photoluminescence spectra of the 60Leu40Dio5Bi glass before (a) and after (b) the crystallization. Photoluminescence was excited at 470 nm (solid line) and 532 nm (dashed line). The scaling factors for the spectra of crystallized specimens are given relative to the spectra of glass, excited at the same wavelength.

**Fig.3** Photoluminescence spectra of the 20KGaSi<sub>2</sub>O<sub>6</sub> – 1Bi<sub>2</sub>O<sub>3</sub> glass before (a) and after (b) the crystallization. Photoluminescence was excited at 470 nm (solid line) and 532 nm (dashed line). The scaling factors for the spectra of crystallized specimens are given relative to the spectra of glass, excited at the same wavelength.

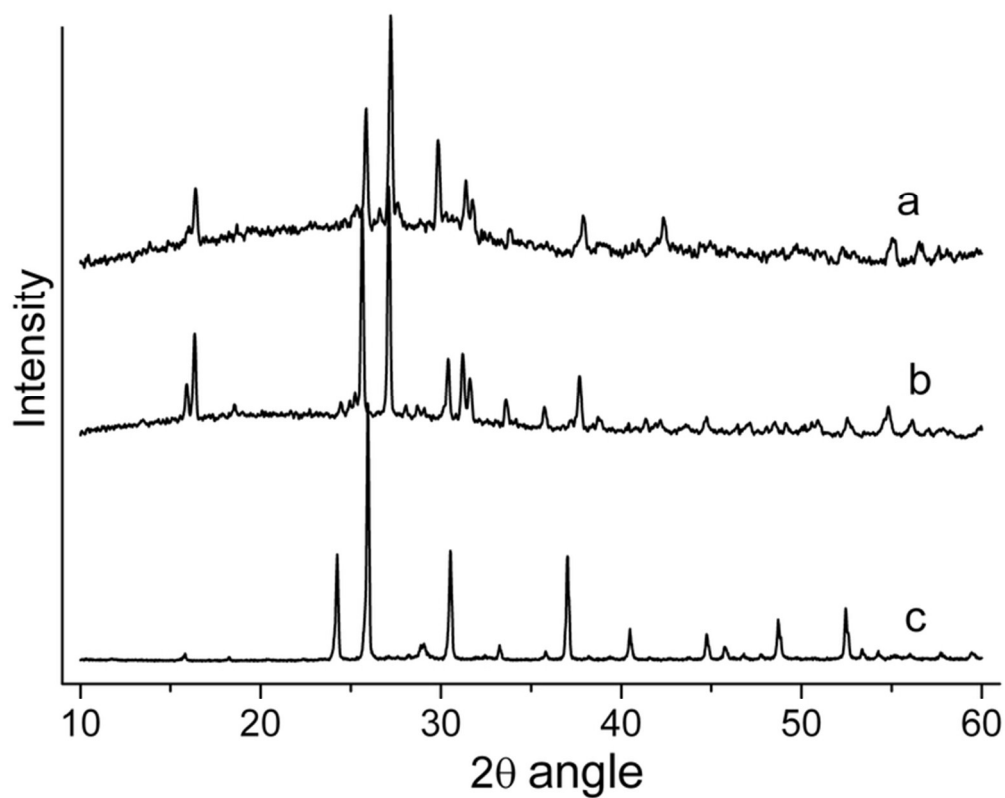
**Fig.4** Photoluminescence spectra of bismuth-doped pollucite, crystallized from the melt with 7CsAlSi<sub>2</sub>O<sub>6</sub>-3B<sub>2</sub>O<sub>3</sub>-1.05Bi<sub>2</sub>O<sub>3</sub> composition. The luminescence was excited at 405 nm (a), 532 nm (b), 635 nm (c), 660 nm (d) and 690 nm (e).

**Fig.5** Photoluminescence spectra comparison for the bismuth-doped pollucite samples, crystallized from the melts with 7CsAlSi<sub>2</sub>O<sub>6</sub>-3B<sub>2</sub>O<sub>3</sub>-xBi<sub>2</sub>O<sub>3</sub> compositions, containing different bismuth oxide amounts (for the solid line x=0.117; for the dashed line x=0.35; for the dot line x=1.05). The luminescence was excited at 405 nm (a), 532 nm (b), 635 nm (c), and 660 nm (d). The intensity was scaled to superimpose the spectra upon one another.

**Fig.6** Photoluminescence decay plots for the bismuth-doped gallium leucite (KGaSi<sub>2</sub>O<sub>6</sub>) specimen, registered at 1150 and 1200 nm ( $\lambda_{\text{ex}}=532\text{nm}$ ). The characteristic decay times, measured at seven different wavelengths are shown in the insert.

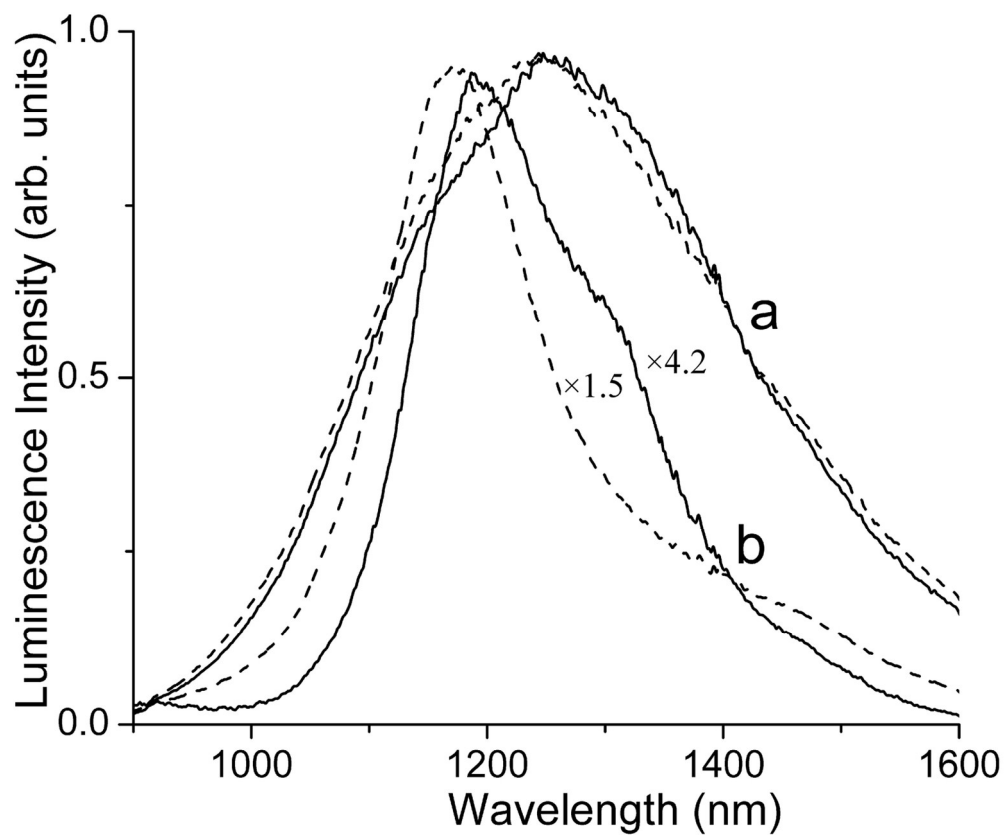
**Fig.7** The influence of the different crystal field strength on the position of the Bi<sup>+</sup> low excited states and NIR photoluminescence wavelengths in the disordered media.

**Fig.8** The dependence of the NIR photoluminescence intensity on the excitation wavelength for the bismuth-doped gallium leucite ( $\text{KGaSi}_2\text{O}_6$ ) specimen. The white color means the brighter emission.

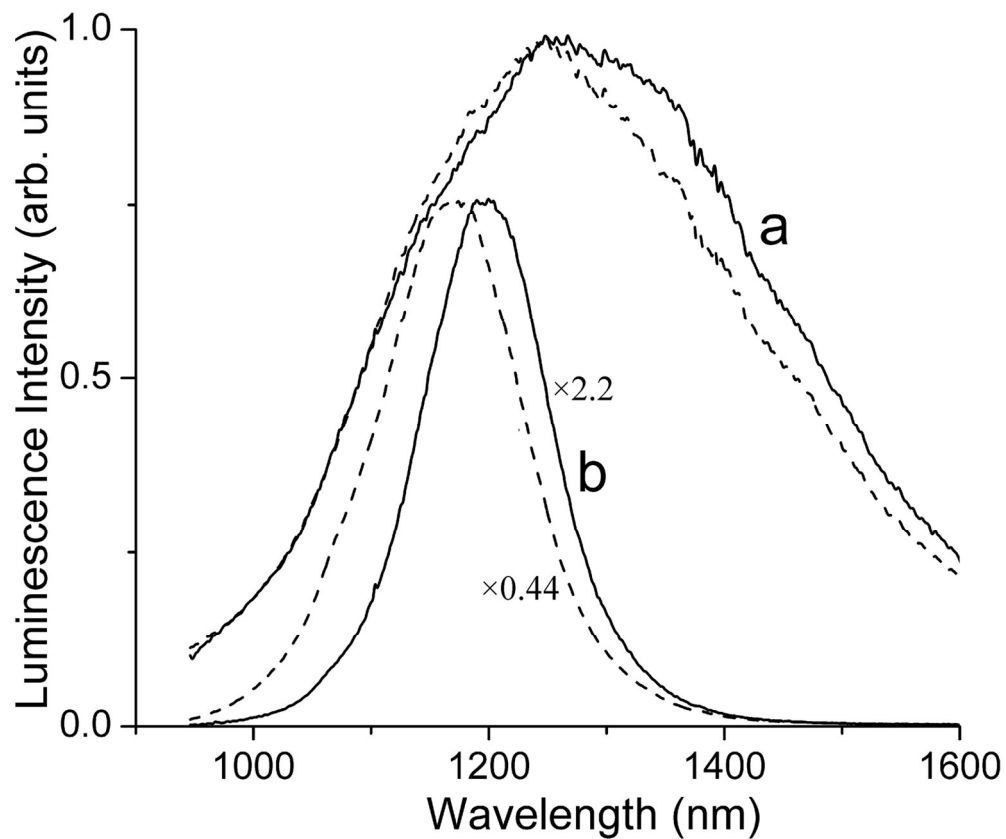


X-ray diffraction patterns of crystallized 60Leu40Dio5Bi glass (a), crystallized 20KGaSi<sub>2</sub>O<sub>6</sub> - 1Bi<sub>2</sub>O<sub>3</sub> glass (b) and pollucite phase, crystallized from the melt with 7CsAlSi<sub>2</sub>O<sub>6</sub>-3B<sub>2</sub>O<sub>3</sub>-1.05Bi<sub>2</sub>O<sub>3</sub> composition and refined from the residual flux by subsequent treatment with KOH and HNO<sub>3</sub> (c). All the noticeable peaks are from leucite (KAlSi<sub>2</sub>O<sub>6</sub>), gallium leucite (KGaSi<sub>2</sub>O<sub>6</sub>) and pollucite (CsAlSi<sub>2</sub>O<sub>6</sub>) phases.

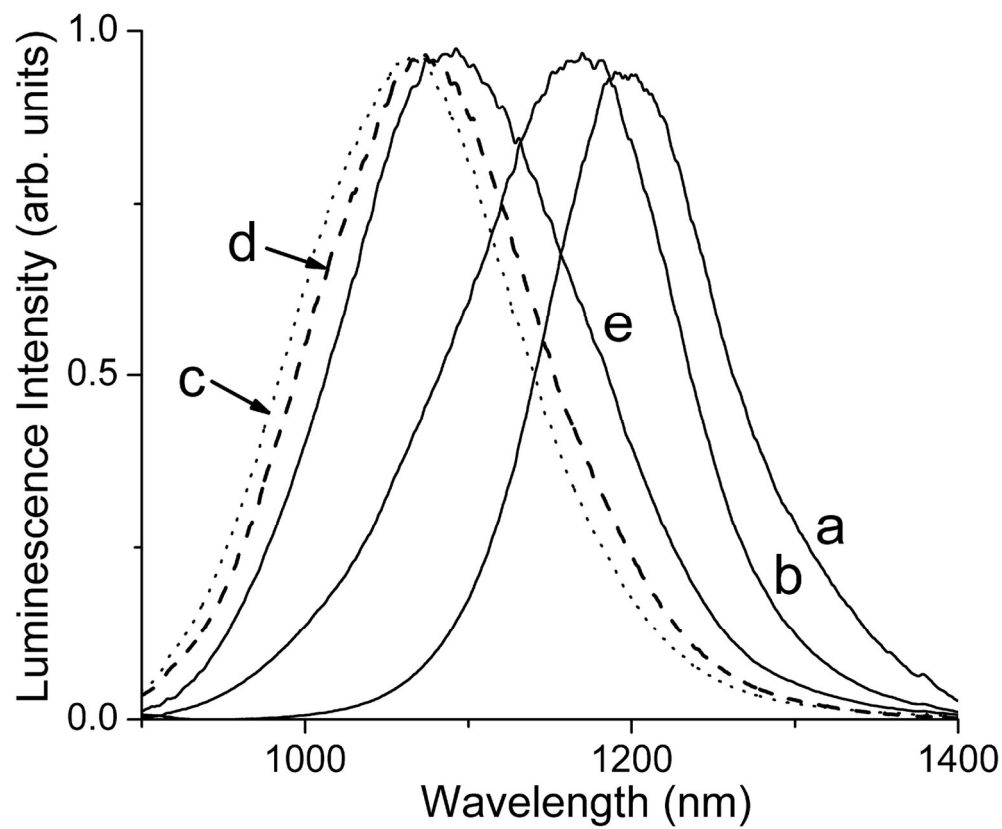
66x53mm (300 x 300 DPI)



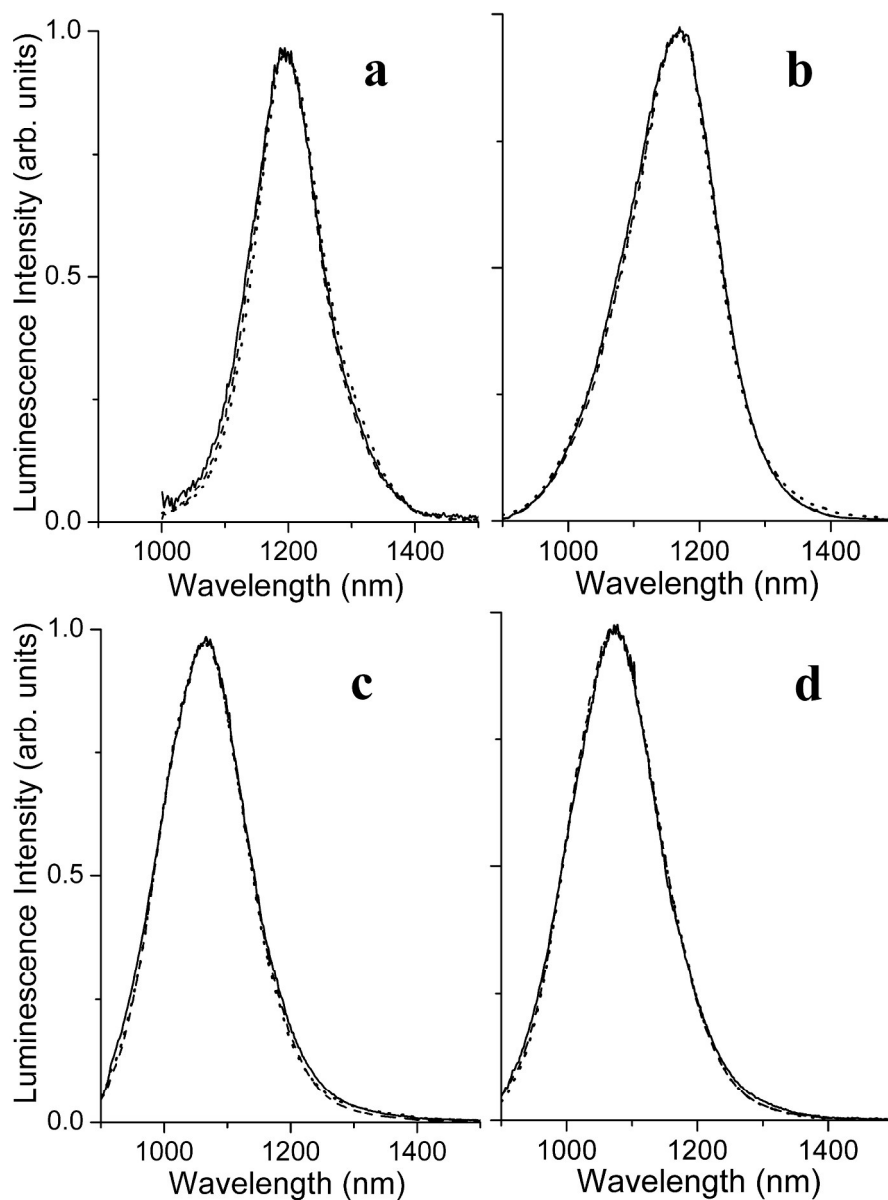
Photoluminescence spectra of the 60Leu40Dio5Bi glass before (a) and after (b) the crystallization. Photoluminescence was excited at 470 nm (solid line) and 532 nm (dashed line). The scaling factors for the spectra of crystallized specimens are given relative to the spectra of glass, excited at the same wavelength. 68x57mm (600 x 600 DPI)



Photoluminescence spectra of the 20KGaSi<sub>2</sub>O<sub>6</sub> - 1Bi<sub>2</sub>O<sub>3</sub> glass before (a) and after (b) the crystallization. Photoluminescence was excited at 470 nm (solid line) and 532 nm (dashed line). The scaling factors for the spectra of crystallized specimens are given relative to the spectra of glass, excited at the same wavelength.  
68x57mm (600 x 600 DPI)

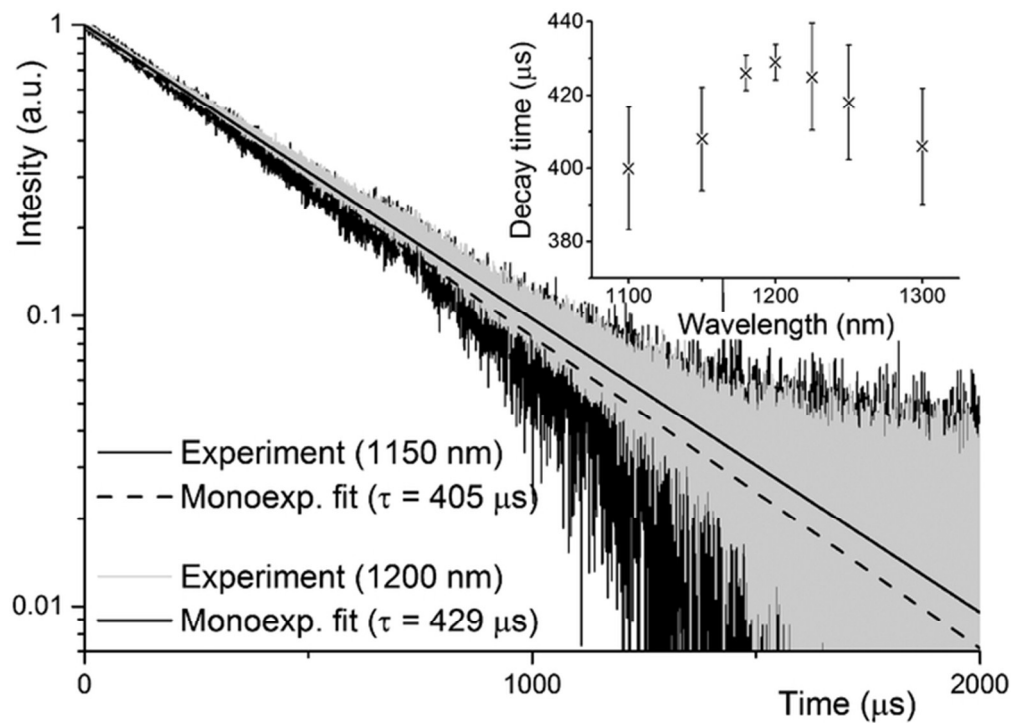


Photoluminescence spectra of bismuth-doped pollucite, crystallized from the melt with  $7\text{CsAlSi}_2\text{O}_6\text{-}3\text{B}_2\text{O}_3\text{-}1.05\text{Bi}_2\text{O}_3$  composition. The luminescence was excited at 405 nm (a), 532 nm (b), 635 nm (c), 660 nm (d) and 690 nm (e).  
68x56mm (600 x 600 DPI)

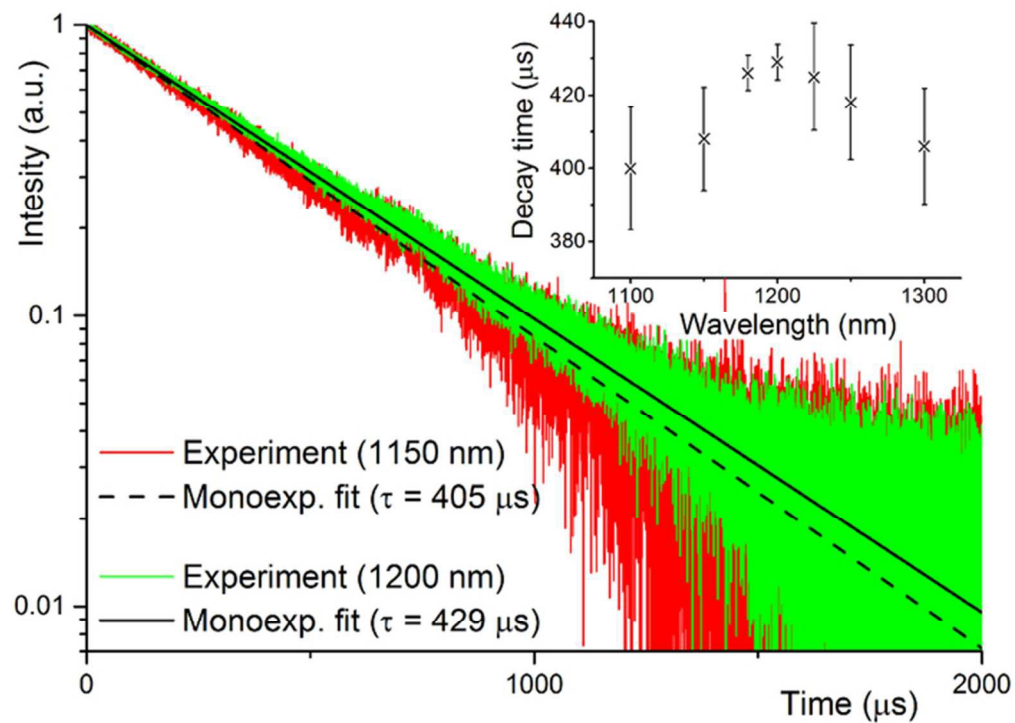


Photoluminescence spectra comparison for the bismuth-doped pollucite samples, crystallized from the melts with  $7\text{CsAlSi}_2\text{O}_6\text{-}3\text{B}_2\text{O}_3\text{-}x\text{Bi}_2\text{O}_3$  compositions, containing different bismuth oxide amounts (for the solid line  $x=0.117$ ; for the dashed line  $x=0.35$ ; for the dot line  $x=1.05$ ). The luminescence was excited at 405 nm (a), 532 nm (b), 635 nm (c), and 660 nm (d). The intensity was scaled to superimpose the spectra upon one another.

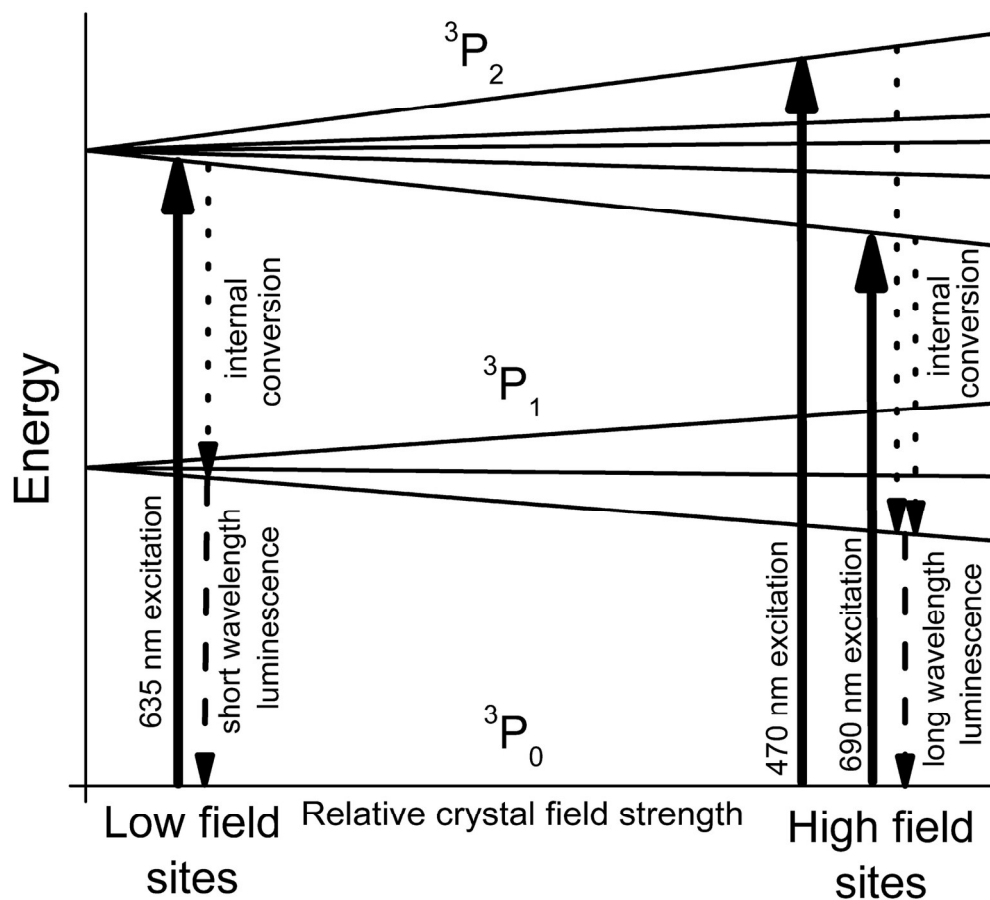
110x148mm (600 x 600 DPI)



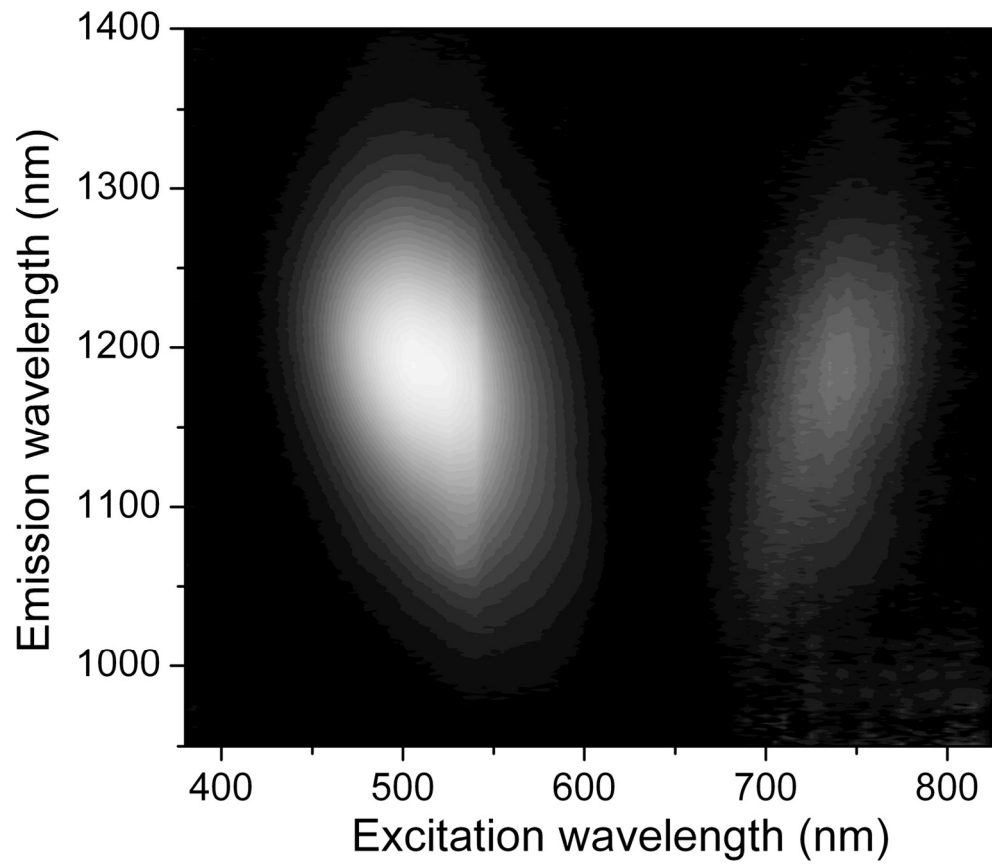
Photoluminescence decay plots for the bismuth-doped gallium leucite ( $\text{KGaSi}_2\text{O}_6$ ) specimen, registered at 1150 and 1200 nm ( $\lambda_{\text{ex}}=532$  nm). The characteristic decay times, measured at seven different wavelengths are shown in the insert.  
59x42mm (300 x 300 DPI)



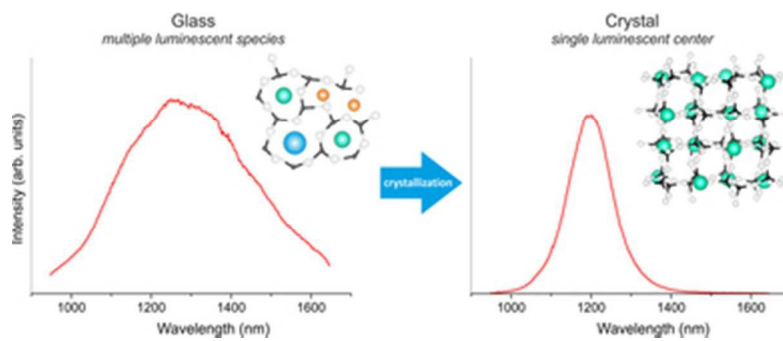
Photoluminescence decay plots for the bismuth-doped gallium leucite ( $\text{KGaSi}_2\text{O}_6$ ) specimen, registered at 1150 and 1200 nm ( $\lambda_{\text{ex}}=532\text{nm}$ ). The characteristic decay times, measured at seven different wavelengths are shown in the insert.  
59x42mm (300 x 300 DPI)



The influence of the different crystal field strength on the position of the Bi<sup>3+</sup> low excited states and NIR photoluminescence wavelengths in the disordered media.  
74x67mm (600 x 600 DPI)



The dependence of the NIR photoluminescence intensity on the excitation wavelength for the bismuth-doped gallium leucite ( $\text{KGaSi}_2\text{O}_6$ ) specimen. The white color means the brighter emission.  
70x60mm (600 x 600 DPI)



33x13mm (300 x 300 DPI)